2018-02-01

Acoustic noise interferometry in a time-dependent coastal ocean

Godin, Oleg A.

Acoustical Society of America

Godin, Oleg A. "Acoustic noise interferometry in a time-dependent coastal ocean." The Journal of the Acoustical Society of America 143.2 (2018): 595-604.
http://hdl.handle.net/10945/61010

Acoustic noise interferometry in a time-dependent coastal ocean[a)]

Oleg A. Godin[b)]
Department of Physics, Naval Postgraduate School, 833 Dyer Road, Monterey, California 93943-5216, USA

(Received 14 September 2017; revised 9 January 2018; accepted 11 January 2018; published online 1 February 2018)

Interferometry of underwater noise provides a way to estimate physical parameters of the water column and the seafloor without employing any controlled sound sources. In applications of acoustic noise interferometry to coastal oceans, the propagation environment changes appreciably during the averaging times that are necessary for the Green's functions to emerge from noise cross-correlations. Here, a theory is developed to quantify the effects of nonstationarity of the propagation environment on two-point correlation functions of diffuse noise. It is shown that temporal variability of the ocean limits from above the frequency range, where noise cross-correlations approximate the Green's functions. The theoretical predictions are in quantitative agreement with results of the 2012 noise interferometry experiment in the Florida Straits. The loss of coherence at high frequencies constrains the passive acoustic remote sensing to exploiting a low-frequency part of measured noise cross-correlations, thus limiting the resolution of deterministic inversions. On the other hand, the passively measured coherence loss contains information about statistical characteristics of the ocean dynamics at unresolved spatial and temporal scales. https://doi.org/10.1121/1.5022287

[JFL] Pages: 595–604

I. INTRODUCTION

Random wave fields that are generated by multiple, spatially distributed, uncorrelated sources maintain coherence at spatial scales which are much larger than the wavelength.[1–8] Time derivative of the cross-correlation function of a diffuse random wave field sampled at two points approximates the Green's functions that describe deterministic wave propagation in opposite directions between the points. This phenomenon was theoretically predicted and experimentally demonstrated for various wave types[1–7,9–11] and underlies the passive remote sensing technique known as noise (or wave) interferometry.[8] In applications of noise interferometry to acoustic oceanography, the feasibility has been demonstrated of passive tomography[12] and thermometry[13] in deep water and passive measurements of current velocity in shallow water.[14] Noise interferometry has been successfully used to probe the seafloor,[15–20] synchronize clocks on autonomous underwater instruments,[14,21–24] and localize acoustic sensors.[21,25,26]

Wind waves, tides, internal gravity waves, turbulence, and other dynamic processes make the ocean a nonstationary acoustic propagation environment. It evolves much faster than in typical seismic applications of noise interferometry. Another important source of nonstationarity in noise interferometry experiments, which is ultimately also a manifestation of ocean dynamics, is motion of acoustic receivers that are installed on moorings[4,12,13,27] or drifters.[29] One might argue that the long-range coherence of diffuse noise, which is theoretically predicted for stationary environments, will be lost when the noise averaging time exceeds a representative time scale of the environmental changes. On the other hand, an argument can be made that small relative changes in amplitudes and travel times of acoustic arrivals should not prevent retrieval of approximate Green's functions. In this paper, we show theoretically that neither of these plausible arguments is valid. Even small environmental changes impart a coherence loss, which tends to increase with propagation range and wave frequency albeit not necessarily monotonically. Rather than preventing passive remote sensing, environment nonstationarity limits from above the range of frequencies, where approximate Green's functions can be retrieved from noise cross-correlations. In shallow water, changes in the sea level are found to have disproportionally large effect on the coherence loss. We will show that the theoretical predictions are in good agreement with results of the 2012 noise interferometry experiment in a coastal ocean off Florida.[27,28]

The 2012 noise interferometry experiment was carried out in the Straits of Florida. Three autonomous, single-hydrophone systems were deployed on the continental shelf approximately along the 100 m isobath 15 km off the Florida Keys. Hydrophones were located 5 m above the seafloor. Horizontal separations were 5.01, 9.76, and 14.76 km for the 1–2, 2–3, and 1–3 hydrophone pairs. About six days of concurrent, continuous records of ambient and shipping noise in the frequency band 10–4000 Hz were obtained on December 13–19, 2012. Averaging times of about 1.5 days were found necessary for an accurate measurement of noise cross-correlation functions at ranges of 50–150 ocean depths. During the measurements, water temperature variations with depth and sound speed gradients were rather weak, with the sound speed $c = 1537.4 \pm 2.4$ m/s throughout the water column. A detailed description of the experiment, including discussions of supporting *in situ* measurements and emergence of approximate Green's functions from measured noise cross-correlations, can be found in Refs. 14, 27, and 28. Specific sound propagation scenarios to be modeled below are largely motivated by the 2012 Florida Straits experiment.

[a)]Parts of this work have been previously reported at the 5th Joint Meeting of the Acoustical Society of America and Acoustical Society of Japan, Honolulu, HI, USA, November–December 2016.

[b)]Electronic mail: oagodin@nps.edu

The remainder of the paper is organized as follows. The effect of random and periodic environmental perturbations on noise cross-correlation functions in shallow-water waveguide is studied theoretically in Sec. II using ray and normal-mode representations of the acoustic field. Effects of several types of time-dependent perturbations in the coastal ocean on empirical Green's functions retrieved from noise cross-correlations are modeled in Sec. III. Dependence of coherence losses of the ray and normal mode components of noise cross-correlations on sound frequency and geometry of the problem is also investigated in Sec. III. Section IV summarizes our findings.

II. COHERENCE LOSS IN A TIME-DEPENDENT OCEAN

A. Noise interferometry in a random medium

Consider a diffuse noise field that is generated by spatially distributed, uncorrelated random sound sources in an environment with time-independent parameters. Let

$$C(\mathbf{R}_A, \mathbf{R}_B, t) = \langle p(\mathbf{R}_A, t_1) p(\mathbf{R}_B, t_1 + t) \rangle_{ns} \tag{1}$$

be the correlation function of the time series of the random acoustic pressure, $p(\mathbf{R}_A, t)$ and $p(\mathbf{R}_B, t)$, that are measured at points $\mathbf{R}_A$ and $\mathbf{R}_B$ in fluid; $\langle \cdot \rangle_{ns}$ denotes averaging over the statistical ensemble of the noise sources. The correlation function is predicted to satisfy

$$\frac{d}{dt} C(\mathbf{R}_A, \mathbf{R}_B, t) = D(t) * [g(\mathbf{R}_A, \mathbf{R}_B, t) - g(\mathbf{R}_B, \mathbf{R}_A, -t)], \tag{2}$$

where $*$ denotes convolution and function $D(t)$ is controlled by the power spectrum of noise sources. For a perfectly diffuse noise field, such as thermal noise, in fluid[1,2,5,6] and fluid-solid[7] environments, $g(\mathbf{R}_A, \mathbf{R}_B, t)$ is the transient Green's function, i.e., the acoustic pressure at $\mathbf{R}_A$ due to an impulsive point source of volume velocity at $\mathbf{R}_B$. The Green's functions $g(\mathbf{R}_A, \mathbf{R}_B, t)$ and $g(\mathbf{R}_B, \mathbf{R}_A, t)$, which describe wave propagation in opposite directions between $\mathbf{R}_A$ and $\mathbf{R}_B$, are identical in motionless environments due to reciprocity and distinct in the presence of fluid flows. In the case of imperfectly diffuse, anisotropic noise field, Eq. (2) is valid asymptotically at sufficiently large separations between $\mathbf{R}_A$ and $\mathbf{R}_B$, and $g(\mathbf{R}_A, \mathbf{R}_B, t)$ is an approximation to the Green's function, which consists of ray and normal-mode arrivals with the same travel time and phase, as in the Green's function, but with amplitudes of the arrivals that depend on noise directionality.[3–5,11,30–32]

Now, consider noise fields in a random medium. The medium is characterized by a set μ of random parameters, which are statistically independent of the set of random noise sources. In every sample of the random medium, define

$$\begin{aligned} E(\mathbf{R}_A, \mathbf{R}_B, t, t_1; \mu) = {} & \frac{d}{dt} [p(\mathbf{R}_A, t_1; \mu) p(\mathbf{R}_B, t_1 + t; \mu)] \\ & - D(t) * [g(\mathbf{R}_A, \mathbf{R}_B, t; \mu) \\ & - g(\mathbf{R}_B, \mathbf{R}_A, t; \mu)]. \end{aligned} \tag{3}$$

Here, E is a random function of receiver positions $\mathbf{R}_A$ and $\mathbf{R}_B$ as well as the time t of measurements at point $\mathbf{R}_A$ and the time delay t_1 between the pressure measurements by the two receivers. In arguments of various functions in Eq. (3), μ indicates that the noise fields and Green's functions refer to a particular realization of the random medium. We assume that a statistical ensemble of noise sources is observed in each sample of the random medium. In each sample of the random medium, averaging over the statistical ensemble of noise sources gives $\langle E \rangle_{ns} = 0$ according to Eq. (2).

Let the noise correlation function be defined as an average over noise sources and variations of environmental parameters: $C(\mathbf{R}_A, \mathbf{R}_B, t) = \langle \langle p(\mathbf{R}_A, t_1) p(\mathbf{R}_B, t_1 + t) \rangle \rangle_{ns}$. Here and below, $\langle \cdot \rangle$ stands for the average over realizations of the random medium. Due to statistical independence of the random noise sources and the environmental variations, the order of averaging does not matter: $\langle \langle \cdot \rangle \rangle_{ns} = \langle \langle \cdot \rangle_{ns} \rangle$. In particular, $\langle \langle E \rangle \rangle_{ns} = \langle \langle E \rangle_{ns} \rangle = 0$ since $\langle E \rangle_{ns} = 0$. We now average Eq. (3) over μ and then over random noise sources. The left-hand side averages to zero, while the average of the product in the first square brackets in the right-hand side of Eq. (3) gives the noise correlation function $C(\mathbf{R}_A, \mathbf{R}_B, t)$. Thus, we find

$$\begin{aligned} \frac{d}{dt} C(\mathbf{R}_A, \mathbf{R}_B, t) = D(t) * \big[& \langle g(\mathbf{R}_A, \mathbf{R}_B, t) \rangle \\ & - \langle g(\mathbf{R}_B, \mathbf{R}_A, t) \rangle \big]. \end{aligned} \tag{4}$$

The right-hand side of Eq. (4) contains averaging only over realizations of the environment, and $\langle g \rangle$ is the mean field due to a deterministic point source. The mean field attenuates with propagation range in a random medium because of energy transfer to the random component of the field.[33,34] For the noise cross-correlation function, Eq. (4) indicates that an evolution of the propagation environment during noise averaging results in a frequency-dependent loss of coherence between the noise fields recorded at spatially separated points. Equation (4) and its derivation remain unchanged if, instead of a random medium, noise fields are measured in an environment with time-dependent parameters as long as the temporal scale of environmental variations is large compared to the acoustic travel time, so that acoustic propagation can be accurately described in the "frozen medium" or quasi-static approximations.[35] Similarly, Eq. (4) also applies when the average over random noise sources is replaced by averaging over time, provided the statistics of the noise sources are not affected by environmental changes during the noise averaging period.

In Sec. II B and Sec. II C below, we quantify the coherence loss under conditions of the 2012 Noise Interferometry Experiment in the Straits of Florida.

B. Mean field in the ray approximation

Here we introduce a Cartesian coordinate system $\mathbf{R} = (x, y, z)$ with horizontal coordinates x and y and vertical coordinate z increasing upward (Fig. 1). All interfaces are parallel to the horizontal plane xy.

Consider a point source in a uniform fluid layer with a sound speed c and density ρ between a free surface $z = H$ and a boundary at $z = 0$, which represents the seafloor. The

boundary is characterized by a plane-wave reflection coefficient V, which is a function of the incidence angle. In the ray approximation, frequency-domain acoustic Green's function is[36]

$$G(\mathbf{R}_A, \mathbf{R}_B, \omega) = \sum_m G_m\,,$$
$$G_m = \frac{\omega\rho}{4i\pi L_m}(-1)^{s_m} V^{b_m} \exp(ikL_m). \tag{5}$$

Here, summation is over the eigenrays connecting the points $\mathbf{R}_A = (x_A,\ y_A,\ z_A)$ and $\mathbf{R}_B = (x_B,\ y_B,\ z_B)$; $s_m = 0,\ 1,\ 2,\ldots$ and $b_m = s_m \pm 1 \geq 0$ are the number of surface and bottom reflections; L_m is the length of the eigenray; ω and $k = \omega/c$ are the wave frequency and wavenumber. Time dependence $\exp(-i\omega t)$ of continuous waves is assumed and suppressed. The time-domain (transient) Green's function $g(\mathbf{R}_A,\ \mathbf{R}_B,\ t)$ can be calculated as the Fourier transform of the frequency-domain Green's function $G(\mathbf{R}_A,\ \mathbf{R}_B,\ \omega)$. The eigenray is straight between surface and bottom reflections (Fig. 1). From simple geometric considerations it follows that

$$L_m = \sqrt{r^2 + (2s_m H \pm z_A \pm z_B)^2}, \quad \theta_m = \arcsin\frac{r}{L_m}, \tag{6}$$

where $r = \left[(x_A - x_B)^2 + (y_A - y_B)^2\right]^{1/2}$ is the horizontal separation of the points $\mathbf{R}_A$ and $\mathbf{R}_B$ and θ_m is the incidence angle of the ray. The signs in front of z_A and z_B in Eq. (6) are positive (negative) when at propagation from $\mathbf{R}_B$ to $\mathbf{R}_A$ the last and, respectively, the first reflection is from the seafloor (from the ocean surface) (Fig. 1).

Let the ocean depth experience small variations around a mean value H_0,

$$H = H_0 + \varepsilon H_1, \quad \langle H_1\rangle = 0, \quad \varepsilon^2\langle H_1^2\rangle = \sigma_H^2. \tag{7}$$

Here, ε is a dimensionless small parameter and $\sigma_H \ll H_0$. When $kr \gg 1$, small changes in environmental parameters affect the acoustic field predominantly through perturbations in the eikonals kL_m. Neglecting small variations in the eigenray amplitudes, from Eqs. (5)–(7) we find

$$G_m = G_{m0}\exp\left[i\varepsilon\omega T_{m1} + i\varepsilon^2\omega T_{m2} + O(\varepsilon^3)\right], \tag{8}$$

where

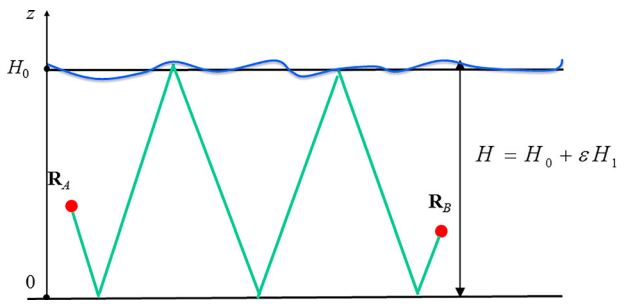

FIG. 1. (Color online) Geometry of the problem. Two hydrophones are located at points $\mathbf{R}_A$ and $\mathbf{R}_B$ in a shallow-water waveguide. Water depth H varies in time due to tides and wind waves on the ocean surface.

$$T_{m1} = \frac{2s_m(2s_m H_0 \pm z_A \pm z_B)}{cL_{m0}} H_1 = \frac{2s_m H_1}{c}\cos\theta_{m0}\,,$$
$$T_{m2} = \frac{2s_m^2 r^2}{cL_{m0}^3} H_1^2 = \frac{2s_m^2 H_1^2}{cr}\sin^3\theta_{m0}, \tag{9}$$

and θ_{m0}, L_{m0}, and G_{m0} have the meaning of the incidence angle, the length of, and the acoustic field on the mth eigenray in the average, or unperturbed, environment. L_{m0}, θ_{m0}, and G_{m0} are given by Eqs. (5) and (6) with H being replaced with H_0. By using Eq. (6), our derivation takes into account the variation of the incidence angle of the eigenray as long as the number of surface reflections in the perturbed and unperturbed environments is the same. To leading order in ε, εT_{m1} gives the perturbation δT_m in the ray travel time $T_m = L_m/c$, while $\varepsilon^2\langle T_{m2}\rangle$ gives the travel time bias, i.e., the difference in the average travel time and the travel time T_{m0} in the average (unperturbed) environment

$$\langle(\delta T_m)^2\rangle \equiv \sigma_T^2 = \frac{4s_m^2\sigma_H^2}{c^2}\cos^2\theta_{m0} + O(\varepsilon^3)\,,$$
$$\langle T_m\rangle - T_{m0} = \frac{2s_m^2\sigma_H^2}{cr}\sin^3\theta_{m0} + O(\varepsilon^3). \tag{10}$$

Unlike at sound scattering from a rough surface,[37] the travel-time bias is always positive.

At long-range sound propagation, where r is large compared to the ray skip distance $2H\tan\theta_{m0}$, the number of surface reflections

$$s_m \approx 0.5rH_0^{-1}\cot\theta_{m0}. \tag{11}$$

For rays with a fixed angle of incidence, Eq. (10) shows that the travel time bias and variance rapidly increase with the propagation range: $\langle T_m\rangle - T_{m0} \propto r$ and $\sigma_T^2 \propto r^2$. In contrast, for rays with a fixed number of surface reflections, $\langle T_m\rangle - T_{m0} \propto r^{-1}$ and $\sigma_T^2 \propto r^{-2}$. Travel time fluctuations decrease with range for such rays because their grazing angles tend to zero when $r \to \infty$.

To find the average value of the field G_m, we first consider the case where the exponent in Eq. (8) is small compared to unity. By developing the exponential in Eq. (8) in powers of the exponent, averaging, and discarding terms of the third and higher order in ε, we obtain

$$\langle G_m\rangle = G_{m0}\exp\left(i\Phi_2 - 0.5\Phi_1^2\right), \quad \Phi_1 = \omega\sigma_T,$$
$$\Phi_2 = \omega(\langle T_m\rangle - T_{m0}), \tag{12}$$

where Φ_1 and Φ_2 are, respectively, the standard deviation and bias of the wave field phase. The imaginary and real parts of the exponent in Eq. (12) are proportional to the variance σ_H^2 of the ocean depth fluctuations and describe, respectively, the phase difference between the average and unperturbed wave field and attenuation of the mean field due to the ray-travel-time fluctuations.

When the ocean depth perturbations have a Gaussian statistical distribution, one can calculate the average of Eq. (8) in a closed form without the assumption that the travel-time fluctuations are small. Neglecting terms of the fourth and higher order in ε, we obtain

$$\langle G_m \rangle = \frac{G_{m0}}{\sqrt{1-2i\Phi_2}} \exp\left(-\frac{0.5\Phi_1^2}{1-2i\Phi_2}\right). \tag{13}$$

It is easy to check that Eq. (13) reduces to Eq. (12) when $\Phi_1 \ll 1$ and $|\Phi_2| \ll 1$, as expected.

It follows from Eqs. (6) and (10) that $2T_{m0}(\langle T_m \rangle - T_{m0}) = \sigma_T^2 \tan^2\theta_{m0}$, or $2\omega T_{m0}\Phi_2 = \Phi_1^2 \tan^2\theta_{m0}$. Hence, with the exception of very small grazing angles $\pi/2 - \theta_{m0} \sim (\omega T_{m0})^{-1/2}$, the phase differences between $\langle G_m \rangle$ and G_{m0} in Eqs. (12) and (13) are much smaller than amplitude differences, when sound propagates over ranges that are large compared to its wavelength. When the travel-time bias is negligible, $|\Phi_2| \ll 1$ and Eq. (13) simplifies to

$$\langle G_m \rangle = G_{m0} \exp(-\Phi_1^2/2). \tag{14}$$

Hence, the effect of travel-time fluctuations reduces to an exponential attenuation of the mean field. The attenuation rate is proportional to the wave frequency squared. In the case of a single reflection ($s_m = 1$) from a fluctuating boundary, Eqs. (10) and (14) with ${\sigma_T}^2$ from Eq. (10) are consistent with the well-known result for the mean field reflection coefficient[38] derived in the tangent plane approximation.

Some of the results that are derived above for the special case of an acoustic waveguide with a moving upper boundary remain valid under more general conditions. In particular, it is clear from the above reasoning that, whether travel time fluctuations δT_m at long-range propagation are due to fluctuations in the refraction index or geometry of the problem, the mean field attenuation and coherence loss on a particular eigenray are described by Eq. (14) provided the root-mean-square (rms) travel time fluctuations are either small compared to the wave period or have a Gaussian statistical distribution. This result is well known[34] for the mean field of a compact source in an unbounded medium with a fluctuating refraction index.

Moreover, Eqs. (10)–(14) apply also in the case of periodic, rather than random, variations in the environmental parameters. In this case, $\langle\cdot\rangle$ means time averaging over the period of environmental changes. It should be emphasized that, unless the mean field attenuation is weak, the frequency dependence of the latter is not universal and instead contains information about the probability distribution of the environmental fluctuations or, in the case of periodic variations, on their time-dependence. For instance, in the case of harmonic variation of depth with time, when $H = H_0 + 2^{1/2}\sigma_H \cos\Omega t$, assuming $|\Phi_2| \ll 1$ and neglecting terms of the third and higher order in ε, we obtain

$$\langle G_m \rangle = G_{m0} J_0(\sqrt{2}\Phi_1), \tag{15}$$

from Eqs. (8) and (9). As expected, Eq. (15) is consistent with Eq. (12) when $\Phi_1 \ll 1$. For moderate and large values of the phase variance, Eq. (15) predicts much smaller coherence losses than Eq. (14).

Equation (10) for the ray travel time variance was obtained assuming that the ocean surface remains horizontal when the ocean depth changes. This is a reasonable assumption, when horizontal spatial scales of the ocean surface elevations are large compared to the propagation range, e.g., for the depth changes due to oceanic tides or changes in the barometric pressure caused by weather systems or atmospheric tides. In the opposite case of small-scale variations, the correlation length of the ocean surface elevations is small compared to the ray skip distance. Then, the travel-time perturbations due to successive surface reflections are uncorrelated. This is typically the case for the surface elevations due to wind waves. The contribution of surface elevations with variance ${\sigma_h}^2$ and a small correlation length into the ray-travel-time variance equals $\tilde{\sigma}_T^2 = 4 s_m \sigma_h^2 c^{-2} \cos^2\theta_{m0} + O(\varepsilon^3)$. It contains s_m instead of ${s_m}^2$ in Eq. (10) for ${\sigma_T}^2$. Note that, when $\Phi_1 = \omega\tilde{\sigma}_T$, our Eq. (14) is consistent with the mean field attenuation due to wind waves, which was first calculated by Clay;[39] see Eqs. (13) and (14) in Ref. 39. When ${\sigma_h}^2 \le {\sigma_H}^2$, the effect of large-scale surface elevations on the travel time fluctuations and the mean field attenuation dominates the effect of small-scale surface elevations on rays with several or many surface reflections.

C. Mean field in the normal mode representation

Consider a range-independent waveguide, where a fluid occupies the half-space $-\infty < z < H$ with a free surface at $z = H$. Sound speed c and density ρ of the fluid are functions of the vertical coordinate z. Neglecting contributions of the continuous spectrum, the frequency-domain acoustic Green's function is given by the sum of normal modes[36]

$$\begin{aligned} G(\mathbf{R}_A, \mathbf{R}_B, \omega) &= \sum_n G_n\,, \\ G_n &= \frac{\omega}{4} f_n(z_A) f_n(z_B) H_0^{(1)}(\xi_n r). \end{aligned} \tag{16}$$

Here, ${H_0}^{(1)}(\cdot)$ is a Hankel function, ξ_n and $f_n(z)$ are the propagation constant and shape function of the nth normal mode, and the shape functions are normalized by the condition

$$\int_{-\infty}^{H} \frac{dz}{\rho(z)} f_n^2(z) = 1. \tag{17}$$

The shape function $f_n(z)$ gives the vertical dependence of acoustic pressure in the nth normal mode.

Fluctuations in the position of the free surface [see Eq. (7)] lead to small perturbations in the mode shape functions and propagation constants. Retaining only the phase perturbations, which accumulate with range, and using an asymptotic expansion of the Hankel function for large arguments,[36] from Eq. (16) we find a relation

$$\begin{aligned} G_n &= G_{n0} \exp\left[i\varepsilon\xi_{n1} r + i\varepsilon^2 \xi_{n2} r + O(\varepsilon^3)\right], \\ \xi_{n1} &= \left(\frac{\partial \xi_n}{\partial H}\right)_{H=H_0} H_1, \quad \xi_{n2} = \left(\frac{\partial^2 \xi_n}{\partial H^2}\right)_{H=H_0} \frac{H_1^2}{2} \end{aligned} \tag{18}$$

between the fields of a normal mode in the perturbed and the average (unperturbed) waveguides in the far field, where $\xi_n r \gg 1$. In shallow-water oceanic waveguides $|\xi_{n1}| = \xi_{n0} O(H_1/H_0)$ and $|\xi_{n2}| = \xi_{n0} O[(H_1/H_0)^2]$, where ξ_{n0} is the propagation

constant in the unperturbed waveguide. The ratios ξ_{n1}/ξ_{n0} and ξ_{n2}/ξ_{n0} are typically frequency-dependent. Note that, in contrast to the assumptions made in the numerical modeling reported in Ref. 40, neither the Green's function nor a modal arrival in the perturbed medium is a time-shifted replica of the Green's function or the modal arrival in the unperturbed medium.

The derivative $\partial\xi_n/\partial H$ and, therefore, the first-order perturbations in Eq. (18) can be calculated analytically in terms of the unperturbed shape functions and propagation constants as follows:[41]

$$\left(\frac{\partial\xi_n}{\partial H}\right)_{H=H_0} = -\frac{1}{2\xi_{n0}\rho(H_0)}\left(\frac{\partial f_{n0}}{\partial z}\bigg|_{z=H_0}\right)^2. \tag{19}$$

Equations (16) and (19) remain valid in the more general case of a fluid-solid waveguide[42] provided the points $\mathbf{R}_A$ and $\mathbf{R}_B$ are situated in a fluid layer $0<z<H$ overlying a solid half-space $z<H$. The solid can be either isotropic or transversally anisotropic with a vertical axis of symmetry. In the fluid-solid waveguide, the normalization condition Eq. (17) should be replaced with

$$\int_0^H \rho^{-1} f_n^2 dz + \frac{\omega}{\xi_n}\int_{-\infty}^0 (\tau_{xz}v_z - \tau_{xx}v_x)dz = 1, \tag{20}$$

where τ_{xx} and τ_{xz} are components of the stress tensor and v_x and v_z are components of the particle velocity $\mathbf{v}=(v_x, 0, v_z)$ in the nth normal mode with the dependence $\exp(i\xi_n x)$ of its field on horizontal coordinates.[42]

Averaging of Eq. (18) for a normal-mode field is analogous to averaging of Eq. (8) for a ray arrival. The results differ only by the values of the phase variance and bias in Eqs. (12)–(15). For normal modes, from Eq. (18) we find

$$\Phi_1 = \left|\left(\frac{\partial\xi_n}{\partial H}\right)_{H=H_0}\right|\sigma_H r, \quad \Phi_2 = \left(\frac{\partial^2\xi_n}{\partial H^2}\right)_{H=H_0}\frac{\sigma_H^2 r}{2}. \tag{21}$$

In contrast to ray arrivals, the normal mode's phase bias is not necessarily positive. It follows from Eq. (21) that $|\Phi_2| \sim \Phi_1^2/\xi_n r \ll \Phi_1^2$ just as in the case of rays with a fixed, nonzero grazing angle (see Sec. II B). The mode phase variance and bias both increase with propagation range but Φ_1^2 becomes large and the mean field is extinguished before the phase bias reaches $O(1)$ values. This justifies using the simpler Eq. (14) for the average field of a normal mode instead of the more complicated Eq. (13).

The results that are obtained in the ray and normal-mode terms are expected to be equivalent for high-order normal modes.[36] To show that this is indeed the case for the coherence loss, we need to demonstrate that the general expression, Eq. (21), for the mode phase variance reduces to the phase variance, Eqs. (10)–(12), of the corresponding ray arrival under assumptions made in Sec. II B. In the simple waveguide considered in Sec. II B, the unperturbed mode shape function $f_{n0} = A\sin[\omega(z-H_0)c^{-1}\cos\theta_{n0}]$ in the water column, and $\xi_{n0} = \omega c^{-1}\sin\theta_{n0}$. Here A is a constant, which is to be determined from the normalization conditions Eq. (17) or Eq. (20), and θ_{n0} is the incidence angle of rays corresponding to the normal mode. In high-order normal modes, the shape function experiences many oscillations in the water column and rapidly attenuates with depth in the ocean bottom. Therefore, integration in Eqs. (17) and (20) can be restricted to $0<z<H$, and ${f_{n0}}^2$ in the integrand can be replaced with its depth-averaged value $A^2/2$, which gives $A^2 = 2{H_0}^{-1}\rho(H_0)$. Then, from Eqs. (19) and (21) we find

$$\Phi_1 = \frac{\omega\sigma_H r\cos^2\theta_{n0}}{cH_0\sin\theta_{n0}}. \tag{22}$$

Comparison of Eq. (22) to Eqs. (10) and (11) shows that the ray and normal-mode considerations indeed give equivalent results for the phase variance and, hence, the mean field attenuation.

Equation (22) indicates that coherence loss increases with propagation range and wave frequency and decreases with increasing θ_{n0}. At fixed frequency, the normal mode's phase speed increases and the angle θ_{n0} decreases with increasing mode order n. This leads to a rapid increase of phase variance with increasing n. As propagation range increases, the mean field is progressively stripped of the higher-order modes.

The frequency f_C, above which a significant coherence loss occurs, can be estimated by requiring that $\Phi_1 = 2^{1/2}$. Then,

$$f_C = cH_0\sin\theta_{n0}/\sqrt{2}\pi\sigma_H r\cos^2\theta_{n0}. \tag{23}$$

According to Eqs. (14) and (15), at this frequency, the mean field is attenuated by the factor e in the case of normally distributed random perturbations and the factor $1/J_0(2) \approx 4.47$ in the case of a harmonic time variation of the ocean depth. Under conditions of the 2012 Florida Straits experiment, incidence angles of normal modes were larger than about 60°, see Ref. 27, and the magnitude of tidal variations of the ocean depth was about ±0.5 m from the mean.[27] With $\sigma_H = 0.5/2^{1/2}$ m, $\theta_{n0} = 60°$, and $H_0 = 100$ m, Eq. (23) gives $f_C \approx 68$ Hz at $r = 5$ km, which is in a good agreement with the empirically determined value[27] $f_C = 70$ Hz. For the reasons explained in Sec. II B, wind waves, which had a similar or smaller surface elevation variance, made a negligible contribution to the coherence loss compared to the tidal contribution.

The normal mode attenuation in the mean acoustic field due to tidally induced ocean depth variations is described by Eq. (14) for Gaussian random variations and Eq. (15) for harmonic depth variation in time. In these equations, the rms phase fluctuations Φ_1, Eq. (21), is proportional to the propagation range r. Our results should be contrasted with the predictions of exponential attenuation of normal modes,[39,43–48] which is equivalent to the propagation constants of the normal modes of the mean field having an imaginary part. The exponential attenuation is obtained under implicit[43,44] or explicit[39,45–48] assumption that the correlation length of the random variations of the waveguide's parameters is small compared to the skip distance of the ray that corresponds to the normal mode. As discussed in Sec. II B, our analysis also gives exponential attenuation in the case of a small

correlation length provided phase fluctuations are either Gaussian or weak. When the correlation length of the ocean depth variations is on the order of the propagation range or larger, as is the case for tidally induced depth changes in the 2012 noise interferometry experiment in the Florida Straits, the normal mode attenuation in the mean field cannot be described by any complex mode propagation constant ξ_n. Potentially, this can be used to distinguish between contributions of tides and sound absorption in the bottom into the observed coherence loss.

III. LOSS OF NOISE COHERENCE IN A PEKERIS WAVEGUIDE WITH A TIME-DEPENDENT OCEAN SURFACE

In this section, the theory developed in Sec. II is applied to a Pekeris waveguide, which serves as a simple model of the coastal ocean. We consider cross-correlations of diffuse noise recorded by two near-bottom hydrophones in a waveguide with a homogeneous water layer overlying a homogeneous fluid half-space, which represents the ocean bottom. Water depth varies in time and possibly spatially. Spatial scales of the ocean surface variations are either large (tides) or small (wind seas) compared to the horizontal separation r of the hydrophones. The noise averaging time that is used to retrieve empirical Green's functions from two-point correlation function of noise is large compared to the representative time scale of the ocean surface variations. In the simulations presented below, the choice of specific parameters of the waveguide, time-dependent ocean surface perturbations, and propagation ranges is motivated by the environmental conditions and geometry of the 2012 noise interferometry experiment in the Straits of Florida.[14,27]

We characterize effects of the ocean time-dependence on ray and normal mode arrivals in the empirical Green's functions by the ratio

$$K = |K| \exp(2\pi i\kappa) = \langle G_m \rangle / G_{m0}. \tag{24}$$

Here $|K| \le 1$ and $-0.5 \le \kappa \le 0.5$; $|K|$ has the meaning of amplitude of the contribution of mth ray or normal mode arrival into the empirical Green's function relative to its contribution in the case of stationary ocean. The factor $|K|$ quantifies the decrease of signal-to-noise ratio (SNR) in interferometric measurements due time-dependent perturbations. The SNR decrease is generally accompanied by a phase distortion, which is quantified by κ. When $K = 1$, there are no coherence losses and no phase distortions; $K = 0$ represents the total loss of coherence.

Figure 2 illustrates effects of large- and small-scale ocean surface perturbations on ray arrivals as predicted by Eqs. (10), (14), and (15). Tides result in a much bigger loss of coherence than wind waves with the same rms amplitude, even for rays with as few as five surface reflections [Fig. 2(a)]. For random surface elevations with Gaussian statistics, the coherence loss exhibits a steady and rapid increase with frequency. In contrast, temporally periodic changes in water depth lead to an oscillatory dependence of K on sound frequency [Fig. 2(b)]. The trend of the coherence loss increasing with frequency remains but is much slower than for random Gaussian perturbations. For a given horizontal separation of hydrophones, increase in the incidence angles of rays contributes to a rapid

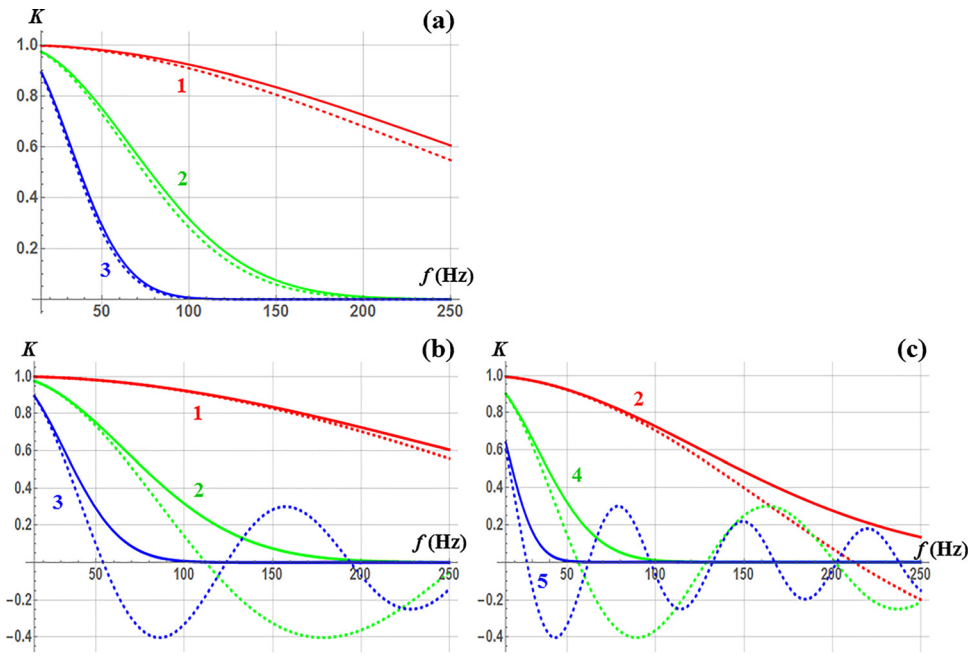

FIG. 2. (Color online) Loss of coherence of surface-reflected ray arrivals in noise cross-correlations. Coherence loss K due to ocean surface motion is shown as a function of sound frequency for rays with different numbers of surface reflections: $m = 5$ (curves marked 1), 10 (2), 15 (3), 20 (4), and 30 (5). Diffuse ambient noise is recorded by near-bottom hydrophones. Average water depth is 100 m; sound speed in water is 1537.4 m/s. (a) The ocean surface varies randomly in time due to tides (solid lines) or tides and wind waves (dashed lines). Gaussian statistics of random surface elevations are assumed. The surface elevations due to tides and wind waves are statistically independent and have rms values of 0.5 m. Horizontal separation of hydrophones is 5 km. (b) Tidal changes in the water depth are either random with Gaussian statistics (solid lines) or periodic with sinusoidal time dependence (dashed lines). The rms values of random and periodic surface elevations is 0.5 m. Horizontal separation of hydrophones is 5 km. (c) Same as in panel (b) but for 10 km horizontal separation of hydrophones.

decrease of coherence with increasing number of surface reflections [Figs. 2(a), and 2(b)]. Comparison of Figs. 2(b) and 2(c) shows that, as expected, for rays with fixed incidence angles, coherence loss increases with propagation range. Simultaneously, oscillations of K with sound frequency become faster for periodic in time surface perturbations. This should lead to stronger distortions of acoustic waveforms at larger horizontal separations of hydrophones.

When ocean surface deviations from the mean with equal amplitude and opposite signs have equal probability, K is real but can become negative [Figs. 2(b) and 2(c)], which is manifested as a switch in polarity of respective ray arrival in the empiric Green's function, mimicking an effect of an extra surface reflection. Values of κ other than 0 and ± 0.5 become possible when positive and negative surface displacements are not symmetric about the mean (Fig. 3).

Non-periodic oscillations of water depth around the mean level occur in a typical situation where solar and lunar tides are present. In Fig. 3, it is assumed that dominant contributions to ocean tides are due to their principle lunar semi-diurnal ($M2$) and principle solar semi-diurnal ($S2$) constituents, which have periods of $T_{M2} = 12.42\,\mathrm{h}$ and $T_{S2} = 12\,\mathrm{h}$ and surface elevation amplitudes A_{M2} and A_{S2}, respectively. Then acoustic travel time perturbation at time t is

$$\varepsilon T_{m1} = \frac{Q}{\omega\sqrt{A_{M2}^2 + A_{S2}^2}}\left[A_{M2}\sin\left(\frac{2\pi t}{T_{M2}}\right) + A_{S2}\sin\left(\frac{2\pi t}{T_{S2}} + \beta\right)\right], \tag{25}$$

$$Q = \frac{2\omega s_m}{c}\sqrt{A_{M2}^2 + A_{S2}^2}\cos\theta_{m0}. \tag{26}$$

according to Eq. (9). Here, β is phase of the solar tide relative to the moon tide at $t = 0$; Q has the meaning of the amplitude of acoustic phase perturbations of the mth ray arrival.

When sound frequency is low or tide amplitudes are small, $Q \ll 1$ and loss of coherence is negligible (Fig. 3). With Q larger than about 0.4, tidal effects are no longer negligible; phase distortion $2\pi\kappa$ and especially the coherence loss $|K|$ become sensitive to amplitudes and the relative phase of tidal components. The phase distortion takes all possible values between $-\pi$ and π but for most acoustic frequencies, κ is close to either 0 or ± 0.5, and $|\mathrm{Im}\,K| \ll |\mathrm{Re}\,K|$. Comparison of Figs. 3(a), 3(b), and 3(c) indicates that empirical acoustic Green's functions carry information about amplitude and modal composition of tides. The initial relative phase β of the tidal components determines whether constructive or destructive interference of the solar and lunar tides is prevalent during the noise observation period. Sensitivity of the empiric Green's function to β is highest when tidal amplitudes A_{M2} and A_{S2} are close [Fig. 3(a)] and lowest when one tidal component dominates [Fig. 3(c)]. If frequency dependencies of the coherence loss and phase distortion were measured for a few ray arrivals, it would provide sufficient information to determine the main components of tides and their amplitudes.

Depending on the amplitude of time-dependent environmental perturbations and the horizontal separation of receivers, coherence losses may prevent retrieval of empirical Green's

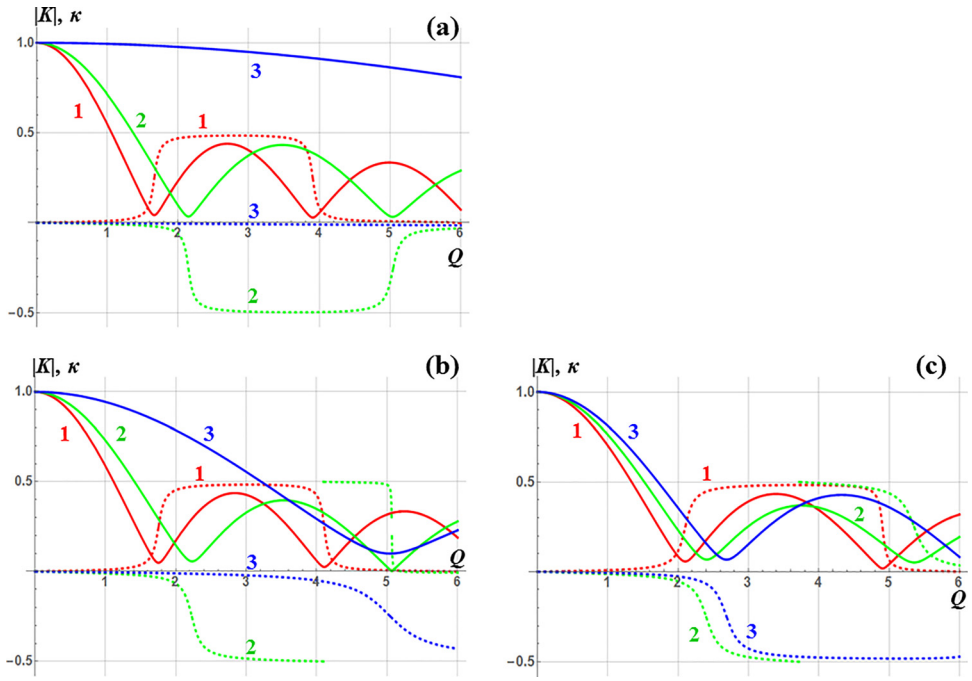

FIG. 3. (Color online) Coherence loss and phase shift of surface-reflected ray arrivals in noise cross-correlations in the presence of a superposition of lunar and solar tides. The coherence loss and phase shift are shown as a function of the amplitude Q, Eq. (26), of the time-dependent phase perturbation in the ray arrival due to tidally induced depth variation. The coherence loss $|K|$ and the phase change $2\pi\kappa$ are calculated assuming different ratios $A_{M2}/A_{S2} = 1$ (a), 2 (b), and 8 (c) of amplitudes of lunar and solar tides and different initial phase shifts of 0 (curves marked 1), $\pi/2$ (2) and π radians (3) between the two dominant tidal components. $|K|$ and κ are shown by solid and dashed lines, respectively. Amplitudes of the lunar and solar tides are assumed to be constant during the noise averaging time of 6 days. For a given incidence angle of a ray, Q is proportional to the acoustic frequency, propagation range, and tide amplitude and inversely proportional to water depth.

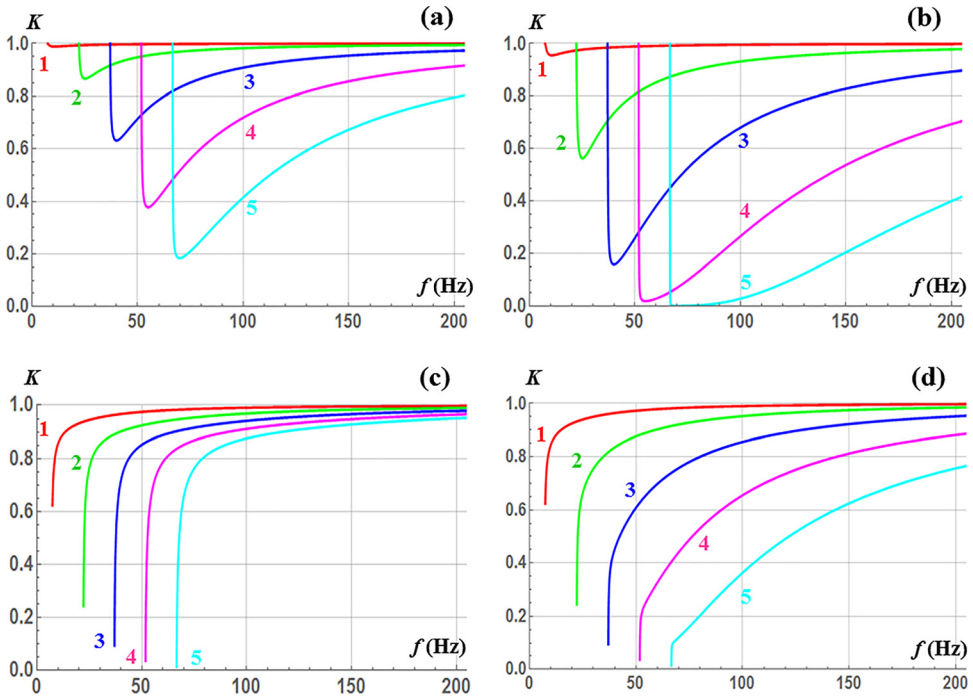

FIG. 4. (Color online) Loss of coherence of normal mode components of noise cross-correlations in a Pekeris waveguide. Coherence loss $|K|$ due to ocean surface motion and sound attenuation in the ocean bottom is shown as a function of sound frequency for five lowest-order normal modes. Each curve is marked by the order $m = 1, 2, 3, 4, 5$ of the respective normal mode. Tidal changes of water depth are modeled as a Gaussian random process with rms elevation of 0.5 m. The following waveguide parameters are assumed in simulations: water depth is 100 m; sound speeds in water and fluid bottom are 1537.4 m/s and 1800 m/s; the ratio of bottom and water densities is 2.2. (a) Coherence loss due to ocean surface motion. Sound attenuation is negligible. Horizontal separation of hydrophones is 5 km in panels (a), (c), and (d). (b) Same as in (a) but for 10 km horizontal separation of hydrophones. (c) Coherence loss due to sound attenuation in the bottom in the absence of tides. Sound attenuation in the bottom is 0.2 dB/wavelength in panels (c) and (d). (d) Combined effect of bottom attenuation and moving ocean surface on the coherence of diffuse noise.

functions from noise cross-correlations at the relatively high frequencies, where the ray approximation is justified. In the normal mode representation of the acoustic field, effects of ocean nonstationarity on noise cross-correlations can be modeled using theoretical results of Sec. II C. These results can be applied, for instance, to determine proper "shading" of normal modes when predicting empirical Green's functions for comparison with observed cross-correlation functions of underwater noise.[20,28] Theoretical predictions of the normal mode coherence loss can be directly compared to experimental measurements when observed noise cross-correlations are separated into their normal mode components[49] using the warping transform.[50,51]

Figure 4 illustrates the influence of time-dependent, large-scale perturbations of the ocean surface, such as tides, on normal-mode components of the noise cross-correlation function. For simplicity, surface elevations are modelled as a Gaussian random process. Similar to ray arrivals [see solid lines in Figs. 2(b) and 2(c)], the coherence loss of individual normal mode components rapidly increases with range [Figs. 4(a) and 4(b)]. The trend of the coherence loss increase with mode order in Figs. 4(a) and 4(b) is similar to the increase in coherence loss with angle of incidence of surface-reflected ray arrivals (Fig. 2). However, frequency dependence of the coherence loss is rather different for rays and normal modes. For Gaussian random surface elevations, the coherence loss steadily increases with frequency (Fig. 2) and, according to Eqs. (10)–(12), scales with frequency and horizontal separation of receivers as ωr. Comparison of Figs. 4(a) and 4(b) clearly shows that there is no such scaling for normal modes. Moreover, the frequency dependence is distinctly nonmonotone, with zero coherence loss at the cutoff frequency and in the high-frequency limit, with a pronounced maximum of the coherence loss at frequencies slightly above the cutoff.

The somewhat unexpected frequency dependence of the coherence loss reflects the sensitivity of the mode phase to water depth variations as represented by the product $r(\partial\xi_n/\partial H)_{H=H_0}$, see Eq. (21). Sound frequency ω and water depth H enter the dispersion relation for phase speeds of normal modes in the Pekeris waveguide only in the combination ωH.[36] Using this fact, it is easy to show that

$$\left(\frac{\partial\xi_m}{\partial H}\right)_\omega = \omega\left(\frac{\partial c_m^{-1}}{\partial H}\right)_\omega = \frac{\omega^2}{H}\left(\frac{\partial c_m^{-1}}{\partial\omega}\right)_H = \frac{\omega}{H}\left(\frac{1}{u_m}-\frac{1}{c_m}\right), \tag{27}$$

where $c_m = \omega/\xi_m$ and $u_m = (\partial\xi_m/\partial\omega)_H^{-1}$ are the phase and group speeds, respectively, of the mth normal mode. The phase speed equals sound speed in the bottom at the cutoff frequency and then steadily decreases with ω to its high-frequency limit, equal to the sound speed in water.[36] The group speed is equal to the bottom sound speed at cutoff, then rapidly decreases with frequency to its minimum value, and after that steadily increases towards the high-frequency limit, which equals the sound speed in water.[36] Equation (27) shows that these well-known properties of phase and

group speeds in the Pekeris waveguide explain the frequency dependence of coherence loss depicted in Figs. 4(a) and 4(b) assuming that sound absorption is negligible.

Attenuation of sound in the bottom leads to exponential decay with range of normal mode amplitudes in both Green's function and the empirical Green's function retrieved from noise cross-correlations. In the Pekeris waveguide, normal mode penetration into the bottom is largest at cutoff and steadily decreases with frequency; at a given frequency, bottom penetration increases with the normal mode order.[36] These properties of normal modes are reflected in the dependencies of their attenuation [Fig. 4(c)] on sound frequency and mode order. Note the sharp contrast between frequency dependencies of the coherence loss due to ocean nonstationarity [Fig. 4(a)] and bottom attenuation [Fig. 4(c)] near the mode cutoff. In a more realistic scenario, where the bottom attenuation and ocean surface nonstationarity are present simultaneously, the two mechanisms of coherence loss combine and, for the waveguide parameters and the hydrophone separation considered, result in the coherence losses that steadily decrease with frequency and increase with mode order [Fig. 4(d)]. Comparison of Figs. 4(a), 4(c), and 4(d) shows that relative significance of the two mechanisms varies depending on ω an m. However, the relative significance of tides vs bottom attenuation always increases with increasing horizontal separation of hydrophones (not shown).

The ray theory predicts that, for each ray arrival, the coherence loss increases with sound frequency, while coherence loss decreases with frequency for each normal mode [Fig. 4(d)]. This apparent contradiction is resolved by noting that, as frequency increases, the number of propagating normal modes grows through addition of higher-order modes with bigger coherence losses.

IV. CONCLUSION

Acoustic noise interferometry relies on the fundamental property of diffuse wave fields, which are generated by a large number of independent sources in a time-invariant medium, to retain coherence at ranges large compared to wavelength. In this paper, we investigated the effect of ocean non-stationarity on the empirical Green's functions that are retrieved from cross-correlations of diffuse ambient and shipping noise. Rapid temporal changes in the environment lead to a frequency-dependent loss of coherence of noise and suppress deterministic features in noise cross-correlations. We quantified the effect of time-dependent environmental perturbations on the ray and normal-mode components of the empirical Green's functions that are measured in noise interferometry experiments. When the noise averaging time is large compared to the representative time scales of random or periodic environmental perturbations, prediction of the resultant coherence loss and phase distortions proved to be closely related to the problem of calculation of the mean field as previously studied in the theory of waves in random media. Equation (4) shows that the environmental information retrievable from measured cross-correlations of diffuse noise is contained in the Green's function of the mean field rather than in the deterministic Green's function in the average (non-perturbed) medium.

In the coastal ocean, the time-dependent processes most relevant to acoustic noise interferometry are changes in the ocean surface geometry. Coherence losses due to ocean surface dynamics are described by Eqs. (13)–(15) and (24). When horizontal separation of receivers is large compared to coastal ocean depth, ocean tides are found to contribute much more to the noise coherence loss than wind waves with comparable amplitudes. The coherence loss is found to have a markedly different range dependence than attenuation due to sound absorption. Equation (23) provides a quick estimate of the frequency, below which noise interferometry can be used for passive acoustic remote sensing of the coastal ocean.

Understanding and prediction of the effects of ocean nonstationarity on the empirical Green's functions is instrumental in planning noise interferometry experiments and interpretation of their results. Further research is necessary to determine whether one can take advantage of the coherence loss in noise cross-correlations to characterize, in a statistical sense, oceanographic processes with times scales that are shorter than the averaging time necessary for emergence of empirical Green's functions from two-point correlations of diffuse noise.

ACKNOWLEDGMENTS

This work was supported in part by the National Science Foundation, Grant No. OCE1657430, and the Research Initiation Program of the Naval Postgraduate School. Helpful discussions with M. G. Brown, W. A. Kuperman, A. G. Voronovich, and N. A. Zabotin are gratefully acknowledged.

[1]S. M. Rytov, "On thermal agitation in distributed systems," Sov. Phys. Dokl. **1**, 555–559 (1956).
[2]R. L. Weaver and O. I. Lobkis, "Diffuse fields in open systems and the emergence of the Green's function," J. Acoust. Soc. Am. **116**, 2731–2734 (2004).
[3]R. Snieder, "Extracting the Green's function from the correlation of coda waves: A derivation based on stationary phase," Phys. Rev. E **69**, 046610 (2004).
[4]P. Roux, W. A. Kuperman, and the NPAL Group, "Extracting coherent wave fronts from acoustic ambient noise in the ocean," J. Acoust. Soc. Am. **116**, 1995–2003 (2004).
[5]O. A. Godin, "Recovering the acoustic Green's function from ambient noise cross-correlation in an inhomogeneous moving medium," Phys. Rev. Lett. **97**, 054301 (2006).
[6]K. Wapenaar, E. Slob, and R. Snieder, "Unified Green's function retrieval by cross-correlation," Phys. Rev. Lett. **97**, 234301 (2006).
[7]O. A. Godin, "Retrieval of Green's functions of elastic waves from thermal fluctuations of fluid-solid systems," J. Acoust. Soc. Am. **125**, 1960–1970 (2009).
[8]K. Wapenaar, D. Draganov, and J. O. A. Robertsson, *Seismic Interferometry: History and Present Status*, SEG Geophysics Reprint Ser. No. 26 (Society of Exploration Geophysicists, Tulsa, OK, 2008).
[9]E. Larose, L. Margerin, A. Derode, B. van Tiggelen, M. Campillo, N. Shapiro, A. Paul, L. Stehly, and M. Tanter, "Correlation of random wavefields: An interdisciplinary review," Geophysics **7**, SI11–SI21 (2006).
[10]K. G. Sabra, E. S. Winkel, D. A. Bourgoyne, B. R. Elbing, S. L. Ceccio, M. Perlin, and D. R. Dowling, "On using cross-correlation of turbulent flow-induced ambient vibrations to estimate the structural impulse response. Application to structural health monitoring," J. Acoust. Soc. Am. **121**, 1987–2005 (2007).

[11]O. A. Godin, N. A. Zabotin, A. F. Sheehan, and J. A. Collins, "Interferometry of infragravity waves off New Zealand," J. Geophys. Res. Oceans **119**, 1103–1122 (2014).
[12]O. A. Godin, N. A. Zabotin, and V. V. Goncharov, "Ocean tomography with acoustic daylight," Geophys. Res. Lett. **37**, L13605, https://doi.org/10.1029/2010GL043623 (2010).
[13]K. F. Woolfe, S. Lani, K. G. Sabra, and W. A. Kuperman, "Monitoring deep-ocean temperatures using acoustic ambient noise," Geophys. Res. Lett. **42**, 2878–2884, https://doi.org/10.1002/2015GL063438 (2015).
[14]O. A. Godin, N. A. Zabotin, L. Zabotina, M. G. Brown, and N. J. Williams, "Passive acoustic measurements of flow velocity in the Straits of Florida," Geosci. Lett. **1**, 16 (2014).
[15]M. Siderius, C. H. Harrison, and M. B. Porter, "A passive fathometer technique for imaging seabed layering using ambient noise," J. Acoust. Soc. Am. **120**, 1315–1323 (2006).
[16]P. Gerstoft, W. S. Hodgkiss, M. Siderius, and C. H. Harrison, "Passive fathometer processing," J. Acoust. Soc. Am. **123**, 1297–1305 (2008).
[17]S. E. Fried, W. A. Kuperman, K. G. Sabra, and P. Roux, "Extracting the local Green's function on a horizontal array from ambient ocean noise," J. Acoust. Soc. Am. **124**, EL183–EL188 (2008).
[18]V. A. Burov, F. V. Grinyuk, V. N. Kravchenko, P. Yu. Mukhanov, S. N. Sergeev, and A. S. Shurup, "Selection of modes from a shallow water noise field by single bottom hydrophones for passive tomography purposes," Acoust. Phys. **60**, 647–656 (2014).
[19]C. Yardim, P. Gerstoft, W. S. Hodgkiss, and J. Traer, "Compressive geoacoustic inversion using ambient noise," J. Acoust. Soc. Am. **135**, 1245–1255 (2014).
[20]X. Zang, M. G. Brown, and O. A. Godin, "Waveform modeling and inversion of ambient noise cross-correlation functions in a coastal ocean environment," J. Acoust. Soc. Am. **138**, 1325–1333 (2015).
[21]K. G. Sabra, P. Roux, A. M. Thode, G. L. D'Spain, W. S. Hodgkiss, and W. A. Kuperman, "Using ocean ambient noise for array self-localization and self-synchronization," IEEE J. Ocean. Eng. **30**, 338–347 (2005).
[22]L. Stehly, M. Campillo, and N. M. Shapiro, "Travel time measurements from noise correlation: Stability and detection of instrumental time-shifts," Geophys. J. Int. **171**, 223–230 (2007).
[23]C. Sens-Schönfelder, "Synchronizing seismic networks with ambient noise," Geophys. J. Int. **174**, 966–970 (2008).
[24]P. Gouédard, T. Seher, J. J. McGuire, J. A. Collins, and R. D. van der Hilst, "Correction of ocean-bottom seismometer instrumental clock errors using ambient seismic noise," Bull. Seism. Soc. Am. **104**, 1276–1288 (2014).
[25]V. V. Goncharov, Yu. A. Chepurin, and O. A. Godin, "Passive acoustic tomography of the ocean using arrays of unknown shape," Acoust. Phys. **59**, 170–178 (2013).
[26]T. Nowakowski, L. Daudet, and J. de Rosny, "Localization of acoustic sensors from passive Green's function estimation," J. Acoust. Soc. Am. **138**, 3010–3018 (2015).
[27]M. G. Brown, O. A. Godin, N. J. Williams, N. A. Zabotin, L. Zabotina, and G. J. Banker, "Acoustic Green's function extraction from ambient noise in a coastal ocean environment," Geophys. Res. Lett. **41**, 5555–5562, https://doi.org/10.1002/2014GL060926 (2014).
[28]M. G. Brown, O. A. Godin, X. Zang, N. A. Zabotin, L. Y. Zabotina, J. S. Ball, and N. J. Williams, "Ocean acoustic remote sensing using ambient noise: Results from the Florida Straits," Geophys. J. Int. **206**, 574–589 (2016).
[29]P. Naughton, P. Roux, R. Yeakle, C. Schurgers, R. Kastner, J. S. Jaffe, and P. L. D. Roberts, "Ambient noise correlations on a mobile, deformable array," J. Acoust. Soc. Am. **140**, 4260–4270 (2016).
[30]K. G. Sabra, P. Roux, and W. A. Kuperman, "Arrival-time structure of the time-averaged ambient noise cross-correlation function in an oceanic waveguide," J. Acoust. Soc. Am. **117**, 164–174 (2005).
[31]O. A. Godin, "Accuracy of the deterministic travel times retrieval from cross-correlations of non-diffuse ambient noise," J. Acoust. Soc. Am. **126**, EL183–EL189 (2009).
[32]O. A. Godin, "Cross-correlation function of acoustic fields generated by random high-frequency sources," J. Acoust. Soc. Am. **128**, 600–610 (2010).
[33]A. Ishimaru, *Wave Propagation and Scattering in Random Media*, Vol. 2. (Academic, New York, 1978).
[34]S. M. Rytov, Yu. A. Kravtsov, and V. I. Tatarskii, *Principles of Statistical Radiophysics. 4: Wave Propagation Through Random Media* (Springer, New York, 1989), pp. 30–32.
[35]O. A. Godin, "Approximate description of sound fields in a time-dependent ocean," Izv. Atmos. Ocean. Phys. **38**, 700–705 (2002).
[36]L. M. Brekhovskikh and O. A. Godin, *Acoustics of Layered Media. 2: Point Sources and Bounded Beams*, 2nd ed. (Springer, Berlin, 1999), pp. 5, 150–152, 166–169, 174–177, 205–208, 312–313.
[37]O. A. Godin and I. M. Fuks, "Travel-time statistics for signals scattered at a rough surface," Waves Random Media **13**, 205–221 (2003).
[38]L. M. Brekhovskikh and Yu. P. Lysanov, *Fundamentals of Ocean Acoustics*, 3rd ed. (Springer, New York, 2003), pp. 203–205.
[39]C. S. Clay, "Effect of a slightly irregular boundary on the coherence of waveguide propagation," J. Acoust. Soc. Am. **36**, 833–837 (1964).
[40]K. F. Woolfe, K. G. Sabra, and W. A. Kuperman, "Optimized extraction of coherent arrivals from ambient noise correlations in a rapidly fluctuating medium," J. Acoust. Soc. Am. **138**, EL375–EL381 (2015).
[41]O. A. Godin, "A note on differential equations of coupled mode propagation in fluids," J. Acoust. Soc. Am. **103**, 159–168 (1998).
[42]O. A. Godin, "Acoustic mode reciprocity in fluid/solid systems: Implications on environmental sensitivity and horizontal refraction," in *Theoretical and Computational Acoustics*, Trieste, Italy (May 10–14, 1999), pp. 59–75.
[43]W. A. Kuperman and F. Ingenito, "Attenuation of the coherent component of sound propagating in shallow water with rough boundaries," J. Acoust. Soc. Am. **61**, 1178–1187 (1977).
[44]P. Ratilal and N. C. Makris, "Mean and covariance of the forward field propagated through a stratified ocean waveguide with three-dimensional random inhomogeneities," J. Acoust. Soc. Am. **118**, 3532–3559 (2005).
[45]F. G. Bass and I. M. Fuks, *Wave Scattering from Statistically Rough Surfaces* (Pergamon, Oxford, 1979), Chap. 11.
[46]C. Penland, "Acoustic normal mode propagation through a three-dimensional internal wave field," J. Acoust. Soc. Am. **78**, 1356–1364 (1985).
[47]A. G. Voronovich, *Wave Scattering from Rough Surfaces*, 2nd ed. (Springer, Berlin, 1999), pp. 209–229.
[48]A. G. Voronovich and V. E. Ostashev, "Mean field of a low-frequency sound wave propagating in a fluctuating ocean," J. Acoust. Soc. Am. **119**, 2101–2105 (2006).
[49]S. N. Sergeev, A. S. Shurup, O. A. Godin, A. I. Vedenev, V. V. Goncharov, P. Yu. Mukhanov, N. A. Zabotin, and M. G. Brown, "Separation of acoustic normal modes in the Florida Straits using noise interferometry," Acoust. Phys. **63**, 76–85 (2017).
[50]G. Le Touzé, B. Nicolas, J. Mars, and J. Lacoume, "Matched representations and filters for guided waves," IEEE Trans. Signal Process. **57**, 1783–1795 (2009).
[51]J. Bonnel and N. R. Chapman, "Geoacoustic inversion in a dispersive waveguide using warping operators," J. Acoust. Soc. Am. **130**, EL101–EL107 (2011).